

# Chapter 5

## Study of the Correlations Between the Dynamics of Thermal Destruction and the Morphological Parameters of Biogenic Calcites by the Method of Thermoprogrammed Desorption Mass Spectrometry (TPD-MS)



**O. G. Bordunova, V. B. Loboda, Y. A. Samokhina, O. M. Chernenko, R. V. Dolbanosova and V. D. Chivanov**

**Abstract** By the method of thermoprogrammed mass spectrometry (TPD-MS) were studied the biogenic calcites thermal desorption spectra (natural limestone chalk, bird eggshells: chicken (*Gallus gallus domesticus*), domestic turkey (*Meleagris gallopavo*), domestic geese (*Anser anser domesticus*), domestic duck (*Cairina moschata*), mollusk shells (*Anadara inaequalis*), and cephalopod fossils Belemnite (*Pachyteuthis Bayle*), as well as calcite nanoparticles. It was shown that the structure of the spectrum correlates with morphological parameters and is a function of samples dispersity degree of biogenic calcites. The increase in the content of nano-, ultra- and microdispersed components in calcite-based biocomposites leads to a significant change in the form of the thermal desorption spectrum, manifested in the appearance of additional temperature desorption areas (peaks) in thermograms and their displacement to lower temperatures area.

---

O. G. Bordunova (✉) · V. B. Loboda · Y. A. Samokhina · R. V. Dolbanosova  
Sumy National Agrarian University, 160, Herasym Kondratiev Str., Sumy 40021, Ukraine  
e-mail: [bordunova\\_olga@Rambler.ru](mailto:bordunova_olga@Rambler.ru)

O. M. Chernenko  
Dnipro State Agrarian and Economic University, 25, S. Efremov St., Dnipro 49600, Ukraine

V. D. Chivanov  
Institute of Applied Physics (IAP), NAS of Ukraine, 58, Petropavlovskaya Str., Sumy 40001, Ukraine

## 5.1 Introduction

The problem of creation on the biomimetic principle of inexpensive and practical nanobiomaterial from common secondary raw materials is a serious challenge for basic and applied researchers [1–3]. The extreme degree of heterogeneity of such materials, which does not make it possible to carry out reliable prognostic calculations of the physicochemical and technological parameters of these materials, still remains only a partially solved problem [2].

A typical example is the still incomplete study of structural features and, as a consequence, the lack of calculated methods for reliable prediction of physicochemical, and especially mechanical, characteristics of biogenic calcite ( $\text{CaCO}_3$ ) [4, 5].

Calcite (chalk, limestone, shells of fossil and living mollusks, the shell of bird eggs and eggs of lizards and snakes) is widely represented in the world around and is also widely used in industry in huge volumes as a building material, absorber-adsorbent of harmful substances in the technologies of protection environment, an effective catalyst in the field of catalytic chemistry, plastic filler, component of electric batteries, etc. [2, 6, 7].

However, there are still no reliable methods for predicting, in particular, the strength characteristics of natural biogenic calcites and their biomimetic analogs [4], which determine the use of various methods of physicochemical analysis to these objects [8].

One of them is a fairly common method of gas analysis—the method of thermoprogrammed desorption mass spectrometry (TPD-MS), which is based on the semi-quantitative determination of gases released from organic/inorganic samples when heated in a programmed mode in vacuum or in the flow of carrier gas [9–13].

The time dependence of the amount of the test gas on temperature (thermogram) is characterized by a complex non-linear character and, as some researchers believe, indirectly reflects the features of the micro- and macrostructures of heterogeneous solid-phase samples [14–17].

Based on the above, the objective of this study was to find possible correlative dependencies between the thermograms obtained in the study of individual biogenic calcites (chalk, bird eggshell, shells of common mollusks, calcite artifacts of fossil cephalopods (belemnites) and micro-macrostructural characteristics of the latter.

Of particular practical importance of research is the need to develop new “green” methods to prevent infectious diseases of agricultural birds during the hatching period [18–21] and to improve the technology for the production of edible eggs, which are characterized by increased strength during transportation and storage [18] as well as the eggshell waste processing of edible eggs (according to rough estimates, all large food concerns daily process more than 1 million eggs [22]).

In the last 25–30 years, the scientific and technical direction, which originally appeared in the physics of thin films, has been rapidly developing, associated with the use of various film nanostructures as functional coatings (film protective coatings) [1–5] and functional elements of micro- and nanoelectronics (film structures with specific electrical and magnetic properties) [6–9]. In the last 25–30 years, the scientific and technical direction, which originally appeared in the physics of thin

films, has been rapidly developing, associated with the use of various film nanostructures as both functional coatings (film protective coatings) [22, 23] and functional elements of micro- and nanoelectronics (film structures with specific electrical and magnetic properties).

## 5.2 Experiment Details

Samples of biogenic calcites were used in the work: (chalk as a typical natural variety of limestone taken from a deposit in the Sumy region; shell of fresh unincubated bird eggs: chicken (*Gallus gallus domesticus*), domestic turkey (*Meleagris gallopavo*), domestic geese (*Anser anser domesticus*), domestic duck (*Cairina moschata*), mollusk shells (*Anadara inaequalis*) and rostra of cephalopod fossils—Belemnite (*Pachyteuthis Bayle*, *Belemnitella Orbigny*).

Temperature-programmed desorption mass spectrometry experiments were carried out with ionization MKh-7304A monopole mass spectrometer (Ukraine) that was adapted for measurements [11, 24]. About 1–5 mg of samples were used for each run. At the beginning of the measurements all samples were degassed to ca.  $5 \times 10^{-3}$  Pa at temperature 20 °C after which they were heated to a temperature of 900 °C. The heating rate was 0.25 °C s<sup>-1</sup>.

Microscopic research was performed using REMMA-102 and REM-106i scanning electron microscopes (Ukraine) and an optical research microscope Carl Zeiss MicroImaging GmbH. For digital processing was used the program Femtoscan (trial version), and for the thermal desorption spectra—software package Origin 8.1.

X-ray diffraction research was performed on X-ray diffractometer “DRON-4M” (Russia).

## 5.3 Results and Discussion

The source experiments were conducted by us with the use of chalk—carbonate sedimentary rock of white color, fine-grained, weakly cemented, soft and crumbly, insoluble in the water, of organic (biogenic) origin. The basis of the chemical composition of chalk is calcium carbonate (91–98.5%) with a small amount of magnesium carbonate, although a non-carbonate part is also present, mainly metal oxides. For natural chalk, the absence of recrystallization and layering is typical. In the chalk column there is a development of large sustained cracks—layered and vertical, filled with chalky flour. On the surface of chalk pieces the network of cracks is strongly condensed. When chalk samples are impregnated with oil, there are hidden wiry structures reveal in the form of interlacing tiny cracks. In all the chalk deposits in different areas (horizons), the chalk differs both in chemical composition and in physical-mechanical properties. In Fig. 5.1 the spectrum of thermal desorption (thermogram) of a chalk sample is shown.

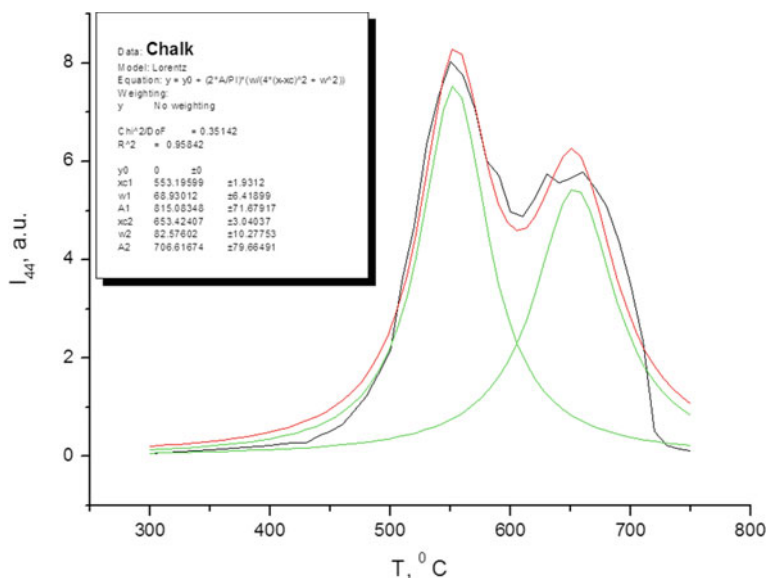


**Fig. 5.1** Thermogram of CO<sub>2</sub> release/release (m/z = 44) by thermal decomposition of sample of chalk; in this Fig. and below the initial thermogram is marked in black (black line), in red—results of curve fitting, in green—result of the total thermogram decomposition into Gaussian curves (Fit Multi-Peaks ⇒ Gaussian)

As can be seen, the release of carbon dioxide CO<sub>2</sub> as a result of the reaction  $\text{CaCO}_3(\text{s}) \rightarrow \text{CaO}(\text{s}) + \text{CO}_2(\text{g})$ , 178 kJ/mol, begins at a temperature of 440–450 °C and ends at 720–750 °C. We note the nonlinear nature of the dependence of the partial pressure of CO<sub>2</sub> in a quartz cell on temperature with two clearly pronounced peaks of 550–560 and 640–660 °C, while the peak in the low-temperature region being significantly higher.

Approximately in the same temperature range of 460–720 °C, takes place the thermal destruction of the sample of the poultry shell (*Gallus gallus domesticus*); however, two pronounced peaks shift to high temperatures 590–610 and 670–690 °C (Fig. 5.2). The thermogram for the sample of the turkey shell is a lot more difficult. Although the range of intense CO<sub>2</sub> emissions is almost identical with the above samples (480–730 °C), the Gaussian decomposition of the total thermal destruction curve showed at least four peaks: 560, 580, 618 and 690 °C (Fig. 5.3). In Fig. 5.4 the thermogram of a domestic geese (*Anser anser domesticus*) domestic goose shell sample is shown, which is characterized by an even more complex dependency between the peaks of intense CO<sub>2</sub> emission and temperature—with interval of an indicated gas release (480–730 °C), using the mathematical processing of the total thermal destruction curve, we can identify six peaks: 520, 560, 600, 660 and 690 °C (Fig. 5.4 shows only two reliable peaks that remain in place with samples changing). A possible explanation for this phenomenon is the increased looseness of the shell of this bird species in combination with an increased amount of the organic component (over

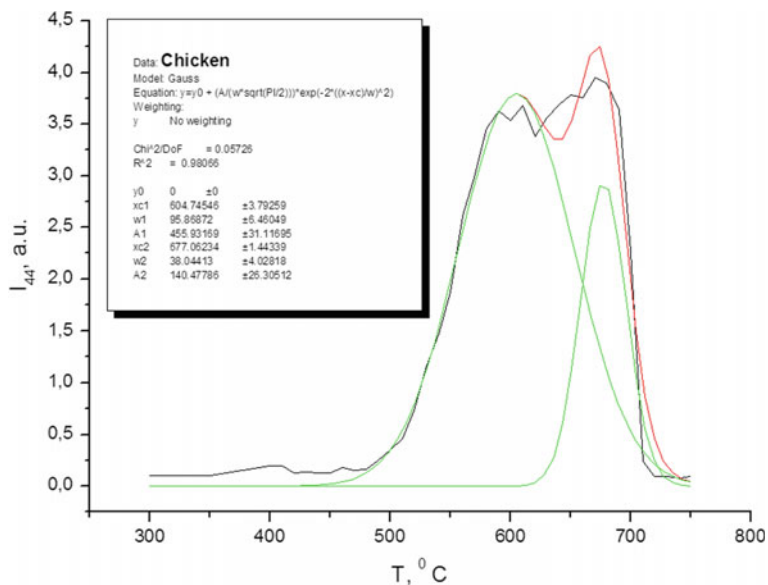


**Fig. 5.2** Thermogram of  $\text{CO}_2$  release/elimination ( $m/z = 44$ ) by thermal decomposition of sample of egg shell chicken (*Gallus gallus domesticus*); unincubated eggs are used in the experiments

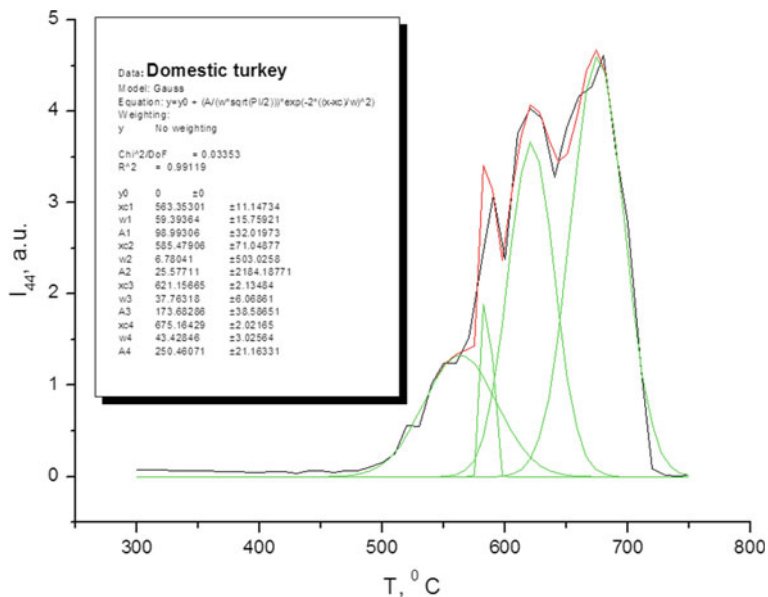


**Fig. 5.3** Thermogram of  $\text{CO}_2$  release/elimination ( $m/z = 44$ ) by thermal decomposition of sample of egg shell domestic turkey (*Meleagris gallopavo*)

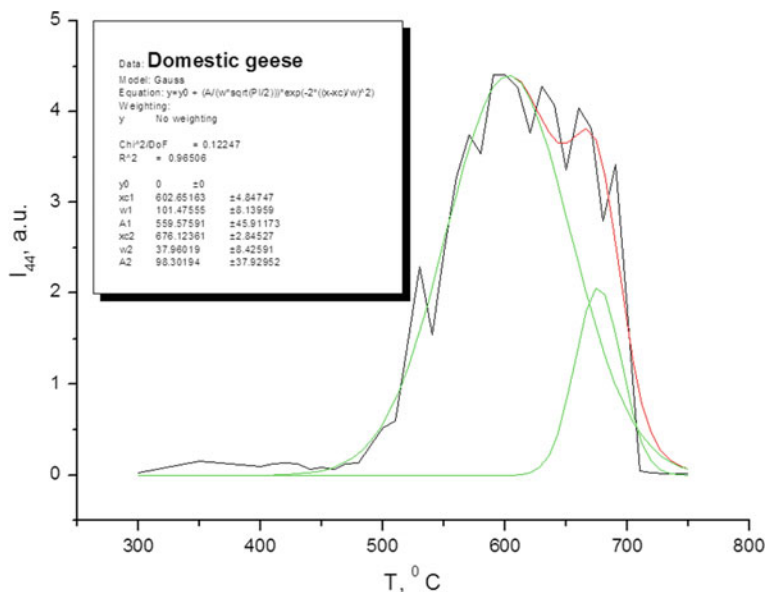


**Fig. 5.4** Thermogram of CO<sub>2</sub> release/elimination ( $m/z = 44$ ) by thermal decomposition of sample of egg shell domestic geese (*Anser anser domesticus*)

shell and membrane shell), as well as carcass “rebar” peptides in the thickness of the shell layer [19, 20]. Direct evidence of this is the result of a digital micrograph processing sample of home goose shells (Fig. 5.5). The nature of the three-dimensional image of the biocrystalline layer of the shell seems to support the increased level of calcite layer disorder.

Finally, in Fig. 5.6 a thermogram of a domestic duck shell sample domestic duck (*Cairina moschata*) is shown. In this case, the peaks of intense CO<sub>2</sub> emission are strongly shifted to the right—to the region of 660, 740 °C.

Summing up the results of all the above experiments, we can conclude that for all dissimilar samples of biogenic calcite while keeping an interval on the temperature scale of 440–750 °C, the intensity and width of the individual peaks constituting the summary thermogram and induced by the intense CO<sub>2</sub> emission is extremely variable. The working hypothesis for explaining this phenomenon was the assumption that the coordinates of the peaks on the temperature scale corresponded to the levels of dispersion of calcite crystals and their location in the biomaterial. Indeed, almost all the studied samples give similar diffraction patterns corresponding to calcium carbonate (Fig. 5.7).

We note that similar, slightly different diffractograms can be obtained from the polarly morphologically different samples of biogenic calcite from the eggshell of domestic chickens (Figs. 5.8, 5.9). If the suggestion about the critical effect of the morphology of a sample of biogenic calcite with the unconditional preservation of the basic crystalline phase (Fig. 5.7) is correct, then experiments with dense samples of

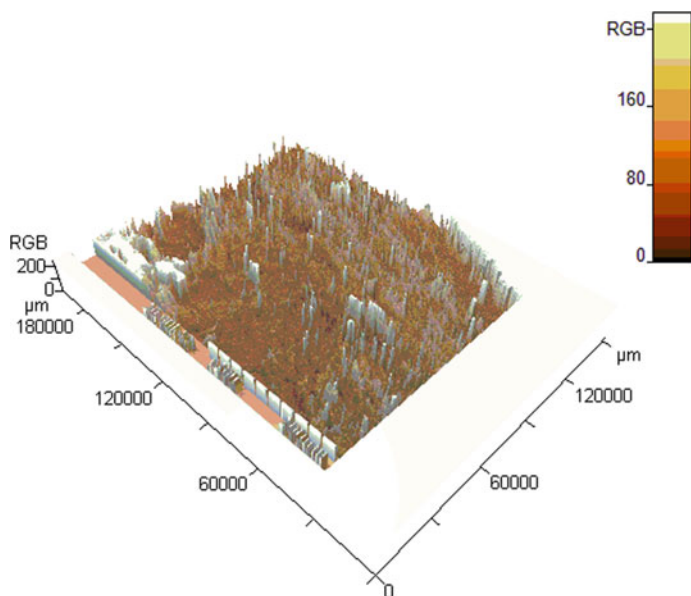


**Fig. 5.5** Digital image of egg shell domestic geese (*Anser anser domesticus*); Femtoscan

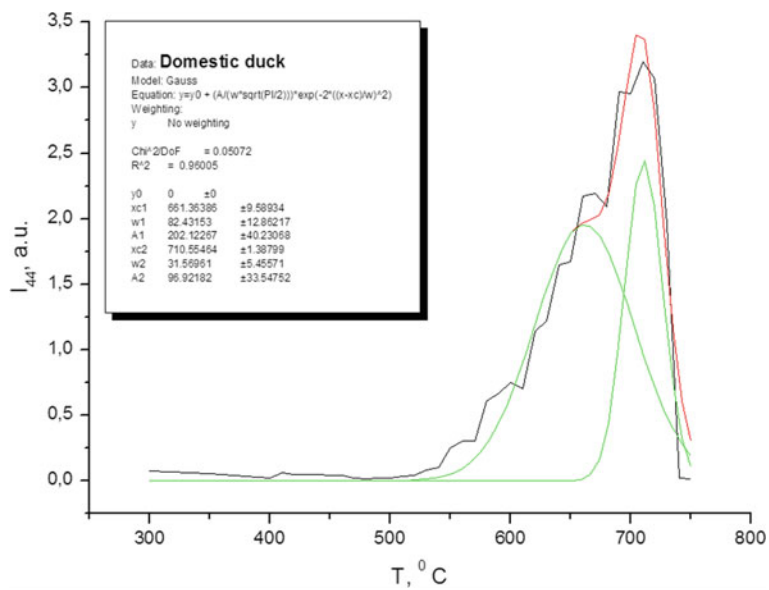


**Fig. 5.6** Thermogram of CO<sub>2</sub> release/elimination ( $m/z = 44$ ) by thermal decomposition of a sample of egg shell domestic duck (*Cairina moschata*)

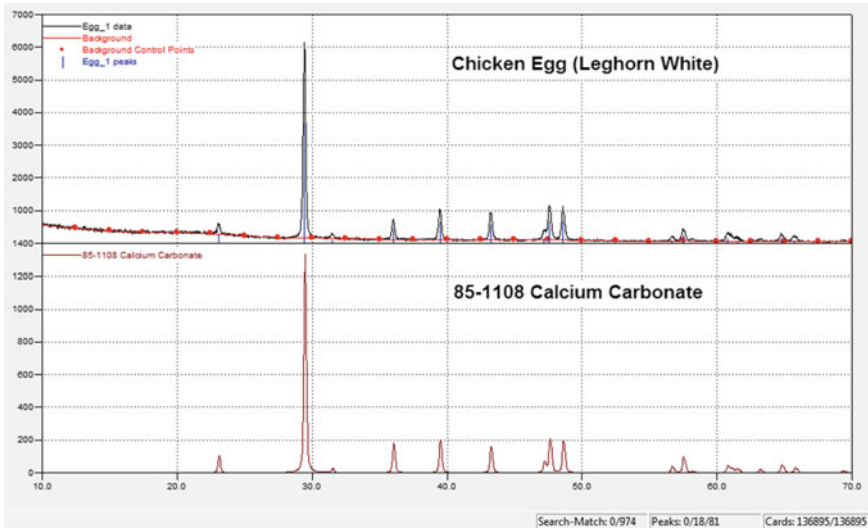
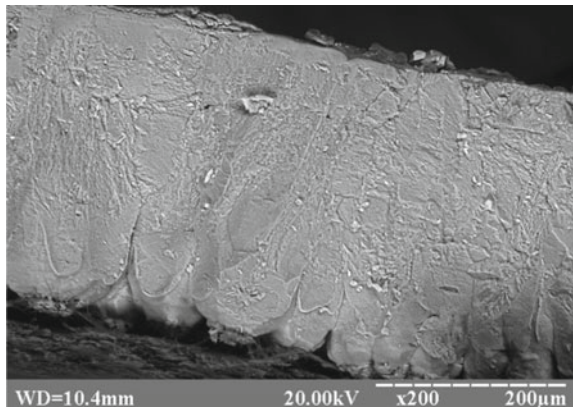


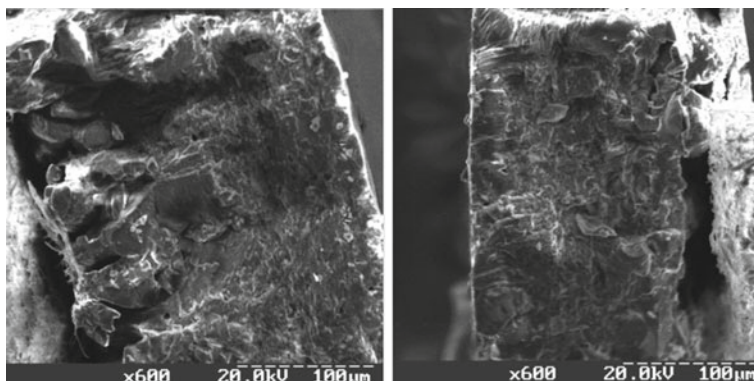
Fig. 5.7 Diffractogram of sample of egg shell chicken (*Gallus gallus domesticus*)

Fig. 5.8 Electron microscopic image of high-quality dense shell of healthy laying hens sample of egg shell chicken (*Gallus gallus domesticus*)



calcite must show a narrowing of the temperature range in which the active release of CO<sub>2</sub> occurs with increasing temperature. Such material we chose a coarse-crystalline calcite material—the fossilized remains of the rosters of belemnites (*Belemnitella Orbigny*).

The roster of the living belemnite served as a kind of internal skeleton. It consisted of radially dispersing needles of calcite. As can be seen from Figs. 5.10 and 5.11, whole and crushed samples of chicken eggshell and belemnite rosters are visually radically different—bird eggs calcite is a very loose conglomerate of CaCO<sub>3</sub> microcrystals, while growth substance is very close to natural crystalline calcite—highly ordered transparent substance. No wonder the thermogram obtained by heating an



**Fig. 5.9** Electron microscopic image of low-quality loose shells of laying hens exposed to stress and infected with infectious diseases sample of egg shell chicken (*Gallus gallus domesticus*)

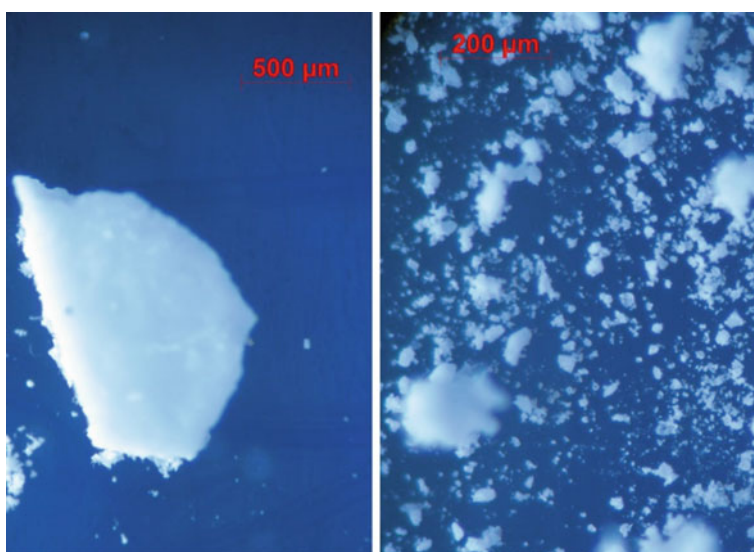


**Fig. 5.10** Micrograph of a sample of the shell of a domestic chicken egg: native shell (left), crushed in a mortar (right) of a sample of egg shell chicken (*Gallus gallus domesticus*)

undivided portion of the crystal sample of the rostra belemnite showed a sharp difference from the similar thermogram for a typical native sample of the eggshells of domestic chicken (Fig. 5.2). On the thermogram of the belemnite sample, a symmetric intense peak is distinguished (range 480–750 °C, peak of 630 °C).

The following suggestion was that for the widening of the temperature range of destruction and an increase in the number of peaks of intense CO<sub>2</sub> emission from chalk and bird egg samples are responsible the heterogeneity of the micro- and

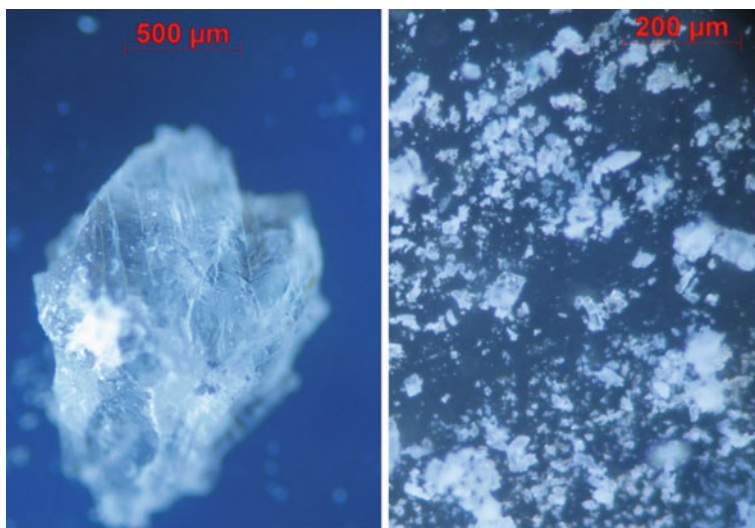


**Fig. 5.11** Micrograph of a belemnite: whole rostrer section (left), rostrum ground in a mortar (right) of sample of belemnite (*Belemnitella Orbigny*)

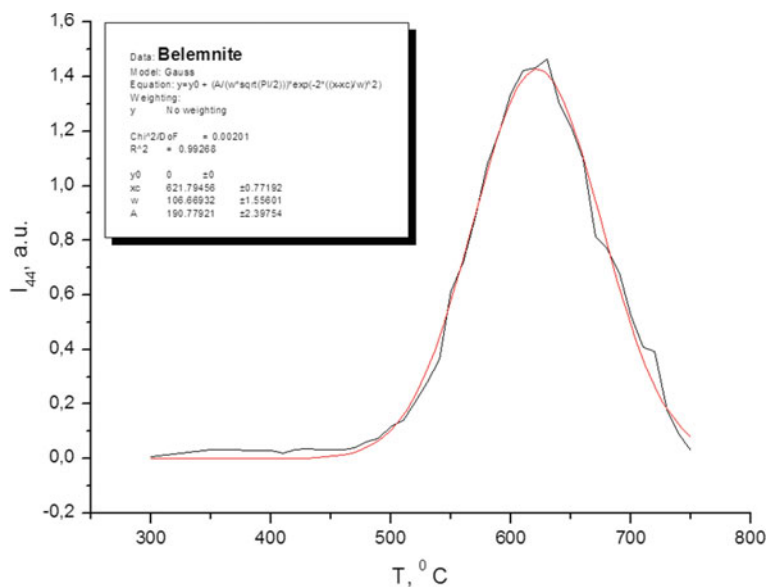


**Fig. 5.12** Thermogram of CO<sub>2</sub> release/elimination ( $m/z = 44$ ) by thermal decomposition of sample of belemnite (*Belemnitella Orbigny*)

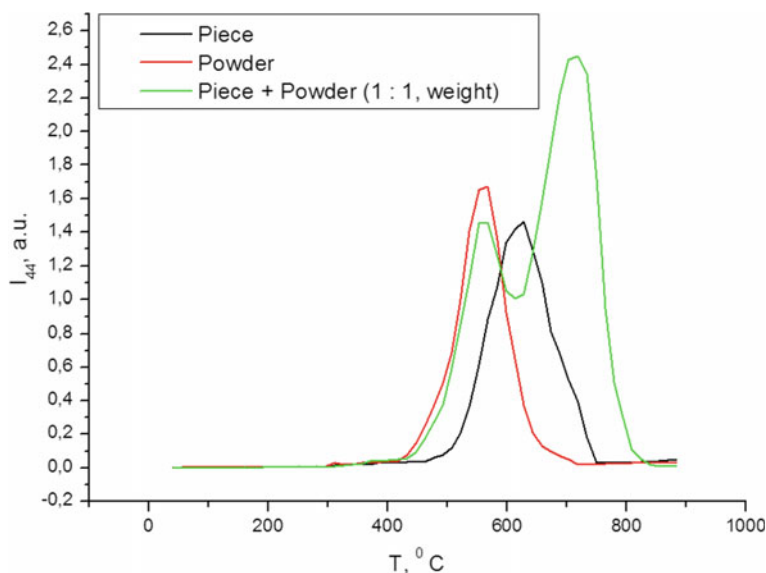


**Fig. 5.13** Thermograms of CO<sub>2</sub> release/elimination ( $m/z = 44$ ) by thermal decomposition of different sample of belemnite (*Belemnitella Orbigny*) **a** piece; **b** powder, **c** piece + powder

macrostructures of calcite-based biocomposites. In this case, the preliminary grinding of the belemnite sample must lead to a change in the type of thermogram, namely, to narrow the destruction interval for fine-grained ( $>5\text{--}10\ \mu\text{m}$ ) and to corresponding widening of the specified interval in the case of combining large- and fine-grained calcite fractions in one sample. As can be seen from Fig. 5.13, the fraction of the crushed sample forms on the thermogram a peak of intense CO<sub>2</sub> emission at 550 °C (control (native whole belemnite)—630 °C), while combining the crushed and native fraction of the sample in one sample leads to a strong widening of the thermogram and the appearance of clearly separated peaks at 550 and 730 °C, which give a good reason for the assumption that the broadening of the temperature ranges of the intense release of CO<sub>2</sub> in the thermograms of biogenic calcites is responsible for their heterogeneity. As can be seen from Fig. 5.14, almost similar results were obtained in the case of the study of the eggshell of domestic chicken (*Gallus gallus domesticus*) (Fig. 5.12).

Finally, the results of the experiment with CaCO<sub>3</sub> nanoparticles obtained using the electrolytic method confirmed our assumptions: a clear high-intensity peak at 520–530 °C was noted on the thermogram (Fig. 5.15).

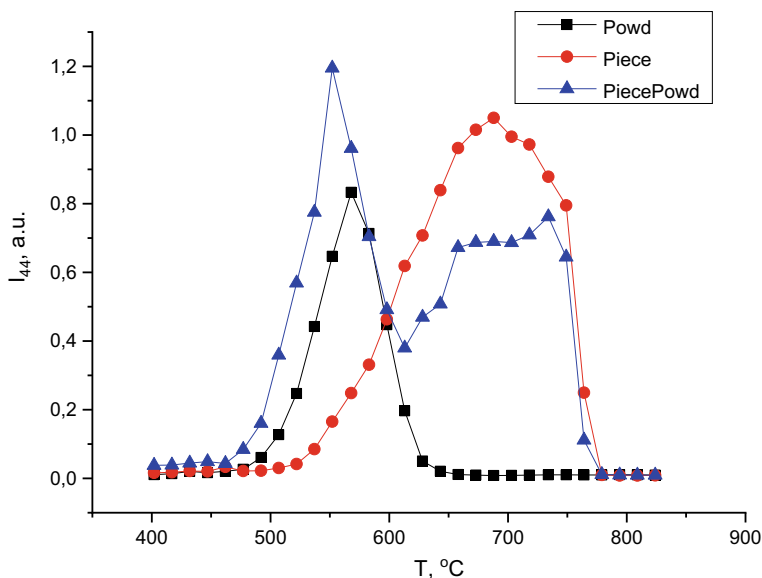


**Fig. 5.14** Thermograms of CO<sub>2</sub> release/elimination ( $m/z = 44$ ) by thermal decomposition of sample of egg shell chicken (*Gallus gallus domesticus*); 1—fine powder; 2—small piece; 3—combination of the small piece and fine powder

## 5.4 Conclusions

By the method of thermoprogrammed desorption mass spectrometry (TPD-MS) were studied the thermal desorption spectra of biogenic calcites (natural limestone chalk, bird egg shells: domestic chicken (*Gallus gallus domesticus*), domestic turkey (*Meleagris gallopavo*), domestic geese (*Anser anser domesticus*), domestic duck (*Cairina moschata*), mollusk shells (*Anadara inaequalvis*) and cephalopod fossil belemnite (*Pachyteuthis Bayle*), as well as calcite nanoparticles. As shown that the spectrum structure correlates with morphological parameters and is a function of the degree of dispersion and samples of biogenic calcites.

An increase in the content of nano-, ultra- and microdispersed components in calcite-based biocomposites leads to a significant change in the form of the thermal desorption graph, occurs in the appearance of additional temperature desorption regions (peaks) and their total displacement to low temperatures area.

Thus, by thermal desorption spectra, obtained by TPD-MS, it is possible to undertake a prior assessment of the morphological parameters (biocrystalline layers degree ordering of biocomposites, the relative content of their components in terms of dispersion degree) of biogenic calcites samples of different origin.

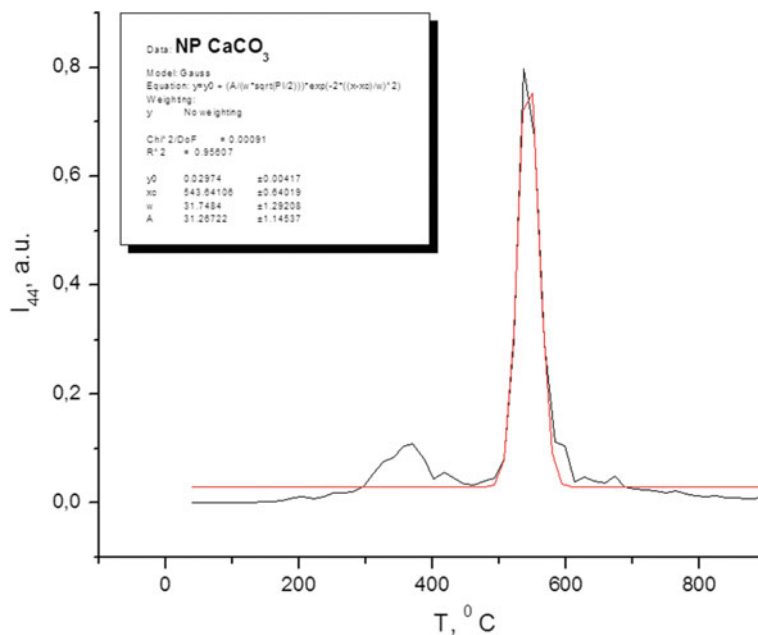


**Fig. 5.15** Thermograms of CO<sub>2</sub> release/elimination ( $m/z = 44$ ) by thermal decomposition of a sample of nanoparticles CaCO<sub>3</sub> (NP CaCO<sub>3</sub>) obtained by electrolytic technique from egg shell chicken (*Gallus gallus domesticus*) (electrolysis media: acetic acid, 20%)

**Acknowledgements** The work has been performed under the financial support of the Ministry of Education and Science of Ukraine (Introduction of nanocomposite materials in innovative technologies for the incubation of poultry eggs; state registration number 0119U100551).

## References

1. K. Endo, T. Kogure, H. Nagasawa, *Biom mineralization: From Molecular and Nano-structural Analyses to Environmental Science* (Springer, Singapore, 2018), p. 413
2. E. Di Masi, L.B. Gower, *Biom mineralization Sourcebook: Characterization of Biom minerals and Biomimetic Materials* (CRC Press, 2014), p. 420
3. A. Shakeel, B. Krishna, I. Saiqa, K. Suvadhan, *Biocomposites: Biomedical and Environmental Applications* (Pan Stanford Publishing, CRC Press, 2018), p. 496
4. J.A.H. Oates, *Lime and Limestone: Chemistry and Technology, Production and Uses* (Wiley-VCH Verlag GmbH, 1998), p. 460
5. R. Zhang, L. Xie, Z. Yan, *Biom mineralization Mechanism of the Pearl Oyster* (Springer, Singapore, 2019), p. 737
6. A. Laca, A. Laca, M. Diaz, Eggshell waste as catalyst: a review. *J. Environ. Management* **197**, 351–359 (2017). <https://doi.org/10.1016/j.jenvman.2017.03.088>
7. P.S. Guru, S. Dash, Sorption on eggshell waste—a review on ultrastructure, biom mineralization and other applications. *Adv. Colloid Interface Sci.* **209**, 49–67 (2014). <https://doi.org/10.1016/j.cis.2013.12.013>

8. J.J. De Yoreo (ed.), in *Methods in Enzymology*, vol 532 (Academic Press, 2013), p. 614
9. V.A. Pokrovskij, Mass spectrometry of the nanostructured systems, *Surface* **2**(17), 63 (2010) (Ukrainian) <https://dspace.nbu.gov.ua/handle/123456789/39323>
10. T.V. Kulik, Use of TPD–MS and linear free energy relationships for assessing the reactivity of aliphatic carboxylic acids on a silica surface. *J. Phys. Chem. C* **116**(1), 570–580 (2012). <https://doi.org/10.1021/jp204266>
11. T.V. Kulik, N.A. Lipkovska, V.N. Barvinchenko, B.B. Palyanytsya, O.A. Kazakova, O.A. Dovbiy, V.K. Pogorelyi, Interactions between bioactive ferulic acid and fumed silica by UV–vis spectroscopy, FT–IR, TPD MS investigation and quantum chemical methods. *J. Colloid Interface Sci.* **339**, 60–68 (2009). <https://doi.org/10.1016/j.jcis.2009.07.055>
12. N. Nastasienko, B. Palianytsia, M. Kartel, M. Larsson, T. Kulik, Thermal transformation of caffeic acid on the nanoceria surface studied by temperature programmed desorption mass-spectrometry, thermogravimetric analysis and FT–IR spectroscopy. *Colloids Interfaces* **3**, 34 (2019). <https://doi.org/10.3390/colloids3010034>
13. T. Hatakeyama, H. Hatakeyama, Thermal properties of green polymers and biocomposites, in *Hot Topics in Thermal Analysis and Calorimetry*, vol 4 (Springer, Netherlands, 2005), p. 336. <https://doi.org/10.1007/1-4020-2354-5>
14. Y. Tsuboi, N. Koga, Thermal decomposition of biomineralized calcium carbonate: correlation between the thermal behavior and structural characteristics of avian eggshell. *ACS Sustainable Chem. Eng.* **6**(4), 5283–5295 (2018). <https://doi.org/10.1021/acssuschemeng.7b04943>
15. C.A.de Araujo Filho, D.Yu. Murzin, A structure sensitivity approach to temperature programmed desorption. *Appl. Catal. A-Gen.* **550**, 48–56 (2018). <https://doi.org/10.1016/j.apcata.2017.11.001>
16. M. Mohamed, S. Yusup, S. Maitra, Decomposition study of calcium carbonate in cockle shell, *Journal of Engineering Science and Technology (JESTEC) School of Engineering, Taylor's University* **7**(1), 1–10 (2012)
17. V.N. Kuznetsov, A.A. Yanovska, S.V. Novikov, V.V. Starikov, T.G. Kalinichenko, A.V. Kochenko, A.G. Ryabyshev, Ya.V. Khyzhnya, S.N. Danilchenko, *J. Nano-Electron. Phys.* **7**(3), 03034 (2015)
18. P.Y. Hester (ed.), *Egg Innovations and Strategies for Improvements* (Elsevier Inc., San Diego, 2017), p. 625
19. M.M. Bain, K. Mcdade, R. Burchmore, A. Law, P.W. Wilson, M. Schmutz, R. Preisinger, I.C. Dunn, Enhancing the egg's natural defence against bacterial penetration by increasing cuticle deposition. *Anim. Genet.* **44**(6), 661–668 (2013). <https://doi.org/10.1111/age.12071>
20. P.W. Wilson, C.S. Suther, M.M. Bain, W. Icken, A. Jones, F. Quinlan-Pluck, V. Olori, J. Gautron, I.C. Dunn, Understanding avian egg cuticle formation in the oviduct: a study of its origin and deposition. *Biol. Reprod.* **97**(1), 39–49 (2017). <https://doi.org/10.1093/biolre/iox070>
21. O. Bordunova, Dissertation, Mykolaiv Agrarian University, 2016
22. M.N. Freire, J.N.F. Holanda, Characterization of avian eggshell waste aiming its use in a ceramic wall tile paste. *Cerâmica* **52**(324) (2006). <https://doi.org/10.1590/s0366-69132006000400004>
23. A.D. Pogrebnjak, O.V. Sobol, V.M. Beresnev, in *Ceramic Engineering and Science Proceedings*, ed. by S. Mathur, S. Sinha Ray, T. Ohji. Nanostructured Materials and Nanotechnology IV, vol 31, (The American Ceramic Society, 2010), p. 127
24. S.N. Danilchenko, V.D. Chivanov, A.G. Ryabishev, S.V. Novikov, A.A. Stepanenko, V.N. Kuznetsov, E.V. Mironets, A.V. Mariychuk, A.A. Yanovska, O.G. Bordunova, A.N. Bugay, The study of thermal decomposition of natural calcium carbonate by the temperature-programmed mass spectrometry technique. *J. Nano-Electron. Phys.* **8**(4), 04031 (2016). [https://doi.org/10.21272/jnep.8\(4\(1\)\).04031](https://doi.org/10.21272/jnep.8(4(1)).04031)